Enabling Technology in High-Baud-Rate Coherent Optical Communication Systems

SI-AO LI[1], **HAO HUANG**[2], (Member, IEEE), **ZHONGQI PAN**[3], (Senior Member, IEEE),
RUNZE YIN[1], **YINGNING WANG**[1], **YUXI FANG**[1], **YIWEN ZHANG**[1],
CHANGJING BAO[2], (Member, IEEE), **YONGXIONG REN**[2], (Member, IEEE),
ZHAOHUI LI[4], **AND YANG YUE**[1], (Member, IEEE)

[1]Institute of Modern Optics, Nankai University, Tianjin 300350, China
[2]Department of Electrical Engineering, University of Southern California, Los Angeles, CA 90089, USA
[3]Department of Electrical and Computer Engineering, University of Louisiana at Lafayette, Lafayette, LA 70504, USA
[4]State Key Laboratory of Optoelectronic Materials and Technologies, School of Electronics and Information Technology, Sun Yat-sen University, Guangzhou 510275, China

Corresponding author: Yang Yue (yueyang@nankai.edu.cn)

ABSTRACT High-baud-rate coherent optical system is essential to support the ever-increasing demand for high-speed applications. Owing to the recent progress in advanced modulation formats, over 1 Tb/s single-carrier data transmission has been achieved in the laboratory, and its commercial application is envisioned in the near future. This paper presented the trend of increasing baud rate and utilizing high-order quadrature-amplitude modulation (QAM), and several enabling technologies in the coherent optical communication systems. We first discussed recent progress of high-order QAM system and digital signal processing technology. Furthermore, we compared the transmission performance of three different ultrahigh-order QAM formats. The paper then reviewed the commonly used methods of achieving over 100 GBaud optically modulated signals. Besides, five attractive modulators and their corresponding modulation structures are illustrated. Key performance parameters including electrode length, 3-dB bandwidth, half-wave voltage, extinction ratio and optical loss are also compared. Finally, the trade-off between the baud rate and QAM orders in implementing high-speed systems are investigated in simulations. The results show that for the coming 800 GbE or 1.6 TbE, PDM-64-QAM might be an idea choice by considering the trade-off between the link reach and required system bandwidth. By adopting the latest probabilistic shaping technology, higher-order QAM signals, such as PS PDM-256-QAM, could be favorable for long reach applications while using extra system bandwidth.

INDEX TERMS Coherent optical communications, high baud rate, QAM, electro-optic modulators.

I. INTRODUCTION

Since Charles K. Kao proposed the feasibility of optical fiber as a light transmission medium in 1966 [1], fiber communication has made tremendous progress over the past half century. During 1990s, wavelength-division multiplexed intensity-modulation and direct-detection (WDM-IMDD) systems dominated the commercial links, due to the emergence of practical erbium-doped fiber amplifier (EDFA) [2], [3]. However, as it is intensity-only modula-

tion, IMDD system has relatively low spectral efficiency (SE), making it difficult to further improve the capacity within the limited bandwidth. Alternatively, coherent optical communication was first investigated in the 1980s, and re-emerged for practical applications in the early 20th century for high SE transmission [4], [5]. Because of its capability to carry multi-dimensional information (e.g. intensity, phase and polarization) and relatively high receiver sensitivity, optical communication systems can transport information with higher speed and extended reach using a single wavelength.

Due to the urgent demand from the emerging large-scale cloud computing, high definition videos and 5G

The associate editor coordinating the review of this manuscript and approving it for publication was San-Liang Lee.

applications, both research and industry communities are exploring ways to further increase the SE and capacity of the optical communication systems. As depicted in Fig. 1, different multiplexing and modulation techniques have been extensively studied to increase the total capacity, including time-division multiplexing (TDM), polarization-division multiplexing (PDM), wavelength-division multiplexing (WDM), quadrature-amplitude modulation (QAM), mode-division multiplexing (MDM) and space-division multiplexing (SDM) [6]–[11]. 100 Gigabit Ethernet (GbE) coherent optical communication systems have been successfully deployed for years, and the 400 GbE standard was also developed in 2017 [12]. In 2019, 400 GbE client-side pluggable optical modules started to flourish, and 400 GbE line-side pluggable modules are expected to debut in 2020. The industry will then be likely marching towards the next generation 800 GbE or even 1.6 TbE. High-baud-rate single-carrier (SC) coherent optical technology is perhaps a key factor to enable this trend.
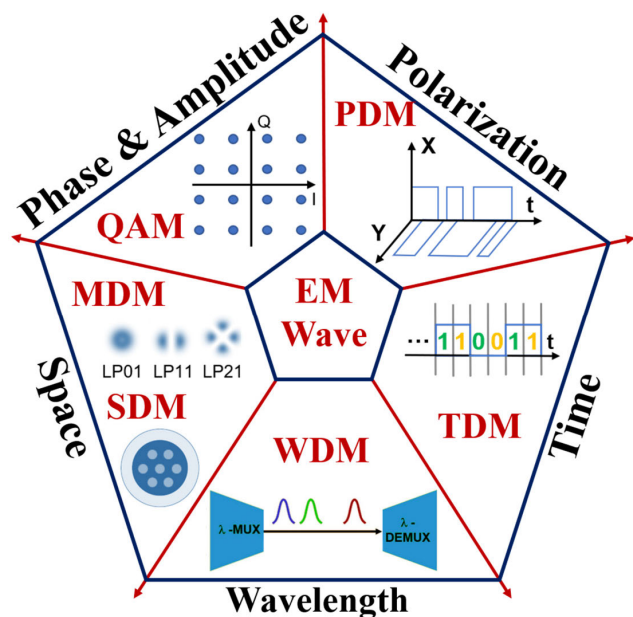

FIGURE 1. Different multiplexing and modulation schemes used in high-speed coherent optical fiber transmission.

For a SC coherent optical system, two options are generally considered to improve the capacity according to:

$$Data\ Rate = Bits\ Per\ Symbol \times Baud\ Rate \quad (1)$$

One is to use high-order QAM formats and the other one is to increase the baud rate of the channel. The first method can improve system capacity together with SE, achieving a given data rate with a lower baud rate and smaller bandwidth. However, higher-order QAM signals require larger optical signal to noise ratio (OSNR) and are less tolerable to phase noise and nonlinear effects. Thus it is more suitable for short reach links. Furthermore, another important parameter that impacts the choice of higher-order QAM is the effective

number of bits (ENOB) of the digital to analog convertor (DAC). Current DACs typically feature 8-bits resolution with an ENOB of less than 6 bits, which is pretty challenging to generate a multi-level signal aiming for ultrahigh-order QAM. In contrast, the second option can adopt a lower-order QAM to mitigate the above-mentioned drawbacks. Nevertheless, higher baud rate means the signal would be more sensitive to chromatic dispersion (CD) and polarization mode dispersion (PMD). Meanwhile, more bandwidths are needed to achieve a given data rate compared to the former method, which means it is limited by the available bandwidth of the optic-electro (OE) and electro-optic (EO) devices.

The growth trend of the baud rates corresponding to different QAM orders is shown in Fig. 2. The data points represent the record-high baud rate of each QAM order over the years. A demonstration of 192 GBaud (GBd) Quadrature Phase Shift Keying (QPSK) is so far the highest baud rate, which was reported in 2019 [13]. It is interesting to see that the baud rates for different QAM orders increase at a pace of around 12 GBd per year. To date, an ultrahigh-order QAM was demonstrated using 3 GBd (72 Gb/s) PDM-4096-QAM over an all-Raman amplified 160 km fiber link with the SE of 15.8 bit/s/Hz [14].
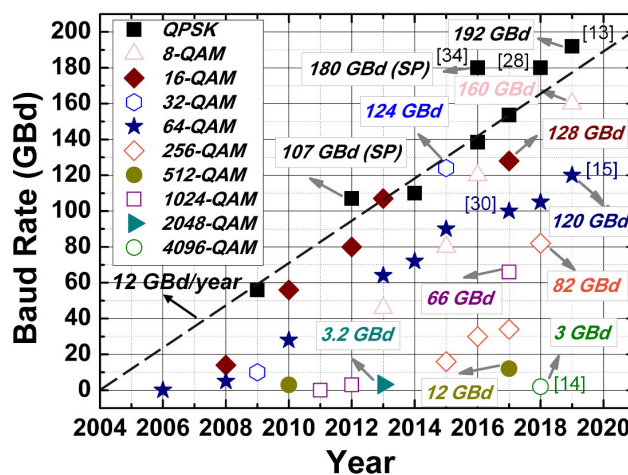

FIGURE 2. Trends for baud rate of different QAM orders (SP: single polarization).

The achievable net SC bit rates over the past decade are also summarized for different QAMs in Fig. 3. According to Fig. 2 and 3, achieving over 100 GBd and 1 Tb/s SC channels with different QAM orders are the frontiers for coherent optical systems. With proper overhead (OH) in the forward error correction (FEC), PDM-64-QAM seems to be a suitable choice to achieve the best trade-off between the baud rate and QAM order to for a 1-Tb/s channel. By using 16.3% OH, the 120 GBd SC probabilistically shaped PDM-64-QAM was achieved with highest 1.04 Tb/s net data rate over three spans of 80 km pure silica core fiber [15]. This paves the ways for the upcoming implementation of 800 GbE and 1.6 TbE, which drives the needs for EO/OE devices with larger bandwidth.
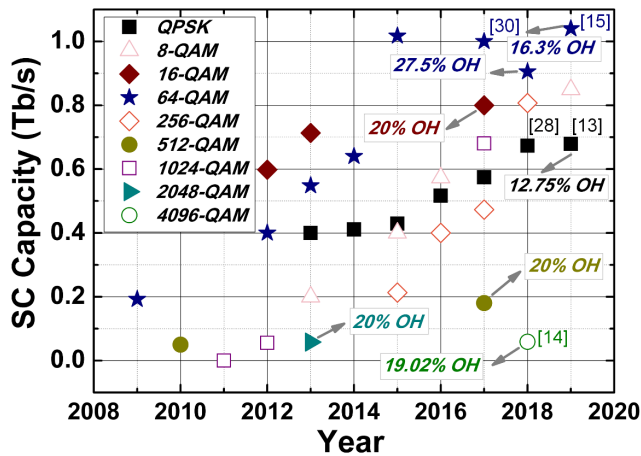
FIGURE 3. Trends for SC capacity of different QAM orders.

The receiver always leads the bandwidth competition with the transmitter. At present, balanced photodiodes (BPDs) can achieve >100 GHz OE bandwidth, which can satisfy the latest needs for high-baud-rate coherent optical communication systems [16]. In contrast, EO modulators face greater challenges, which are thus discussed with more details in this review. The bandwidths of widely used commercial modulators are around 40 GHz, which are not sufficient for the forthcoming above 100 GBd applications [17]. Therefore, the material and structure choices of the modulators are becoming the key parts to realize high-baud-rate coherent optical communication systems.

The rest of the paper is organized as follows: In the next section, a typical setup of the coherent optical system and some common advanced digital signal processing (DSP) algorithms are introduced. Three demonstrated ultrahigh-order QAM signal transmission are also depicted. Next, four commonly used high-baud-rate QAM signal generation methods are summarized. Then, high-efficiency EO modulators are discussed. Five attractive materials are listed and compared in this section. The trade-off between the baud rates and QAM orders for high-speed transmissions are investigated through a series of simulations. The latest probabilistic shaping (PS) technology is also under consideration. Finally, a summary is made for enabling technologies in high-baud-rate systems based on QAM formats.

II. HIGH-ORDER QAM TRANSMISSION

Since 2000, the subject of coherent optical system is moving to high-order QAM formats to get higher channel rates and SE. Until now a QAM-based SC could carry the signals that required an entire WDM setup in 1990s.

A. COHERENT OPTICAL SYSTEM BASED ON QAM FORMATS

A typical coherent optical system scheme based on QAM formats is depicted in Fig. 4. A narrow linewidth laser (typically < 100 kHz) is used to provide a continuous carrier,

and the carrier is divided for two orthogonal polarization modes through a polarization beam splitter (PBS) to achieve PDM. For each polarization mode, two multi-level signals are generated via an arbitrary waveform generator (AWG) after performing transmitter-side (Tx-side) DSP, then coupled to an IQ modulator after amplified to suitable levels. After combined by a polarization beam combiner (PBC), the modulated signals are amplified by an EDFA and transmitted through an optical channel. Then an optical filter is added to filter the out-of-band noise. At the receiver-side (Rx-side), the incoming light is first split by a PBS and mixed with the light from a local oscillator (LO) by a 90-degree hybrid then detected by four BPDs. When the OE conversion is completed, the electrical signal is first filtered by low pass filters (LPF) to mitigate inter-symbol interference (ISI). After performing analog to digital convention, the sampled electrical signal is processed by DSP algorithms for compensation and recovery.

B. ADVANCED DSP ALGORITHMS

Another advantage of the coherent optical systems is the ability to employ a chain of DSP algorithms for low-loss compensation, instead of using separate optical components. A lot of advanced algorithms have been developed for higher baud rate and QAM formats at both the Tx- and Rx-side for pre- and post-compensation. A typical DSP operation procedure for high-baud-rate coherent optical communication systems is given by Fig. 4.

1) TRANSMITTER SIDE
a: PRE-EMPHASIS
The performance of a high-baud-rate high-order QAM signal suffers the distortions from the transmitter bandwidth limitation. Digital pre-emphasis is used to mitigate the bandwidth constraint introduced by EO/OE components [18]. In pre-emphasis, the power of the low-frequency components is decreased to the same as high-frequency components to reduce the effect of high-frequency attenuation in the device frequency response. In generally, the effect of pre-emphasis on the quality improvement for high-baud-rate high-order QAM signals is more pronounced. However, in practice, due to the limited ENOB and bandwidth of the DACs, the performance still gets worse for high-baud-rate coherent optical communication systems with a given QAM order. In such scenarios, a lower-order QAM should be selected to adapt to the limited ENOB, while requiring a higher baud rate. That means for different applications, there is a trade-off among ENOB, baud rate and QAM order.

b: PRE-DISTORTION
The nonlinearity of modulation and amplifier is another obstacle for high-order QAM formats. It is usually introduced by finite extinction ratio of the modulators, total harmonic distortion of the DAC, and material-dependent non-linear phase shift. The pre-distortion is used to overcome the issue by adjusting the level of the incoming signal to
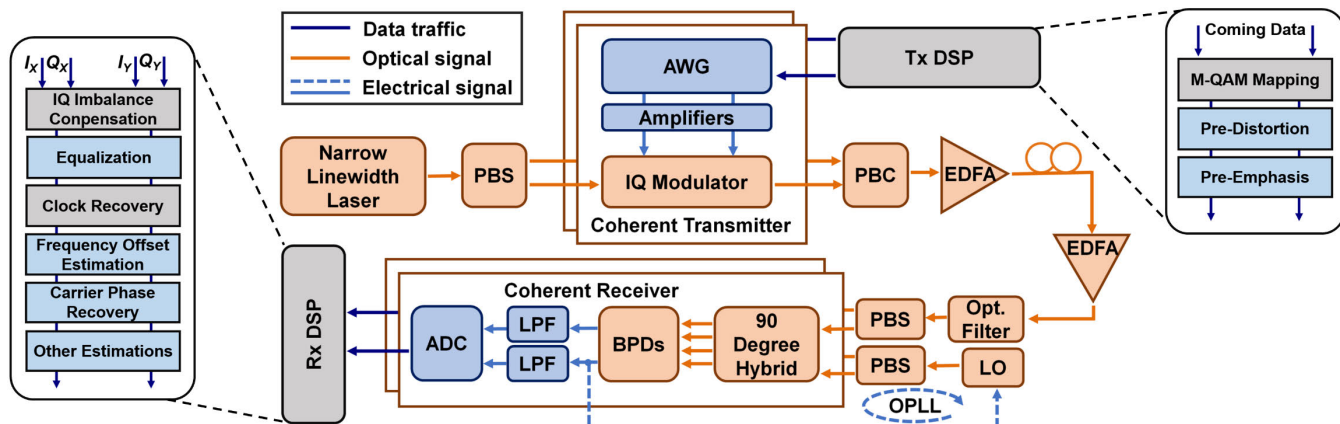
FIGURE 4. The setup of coherent optical system based on QAM formats.

make it suitable for the transfer function of the devices [19]. At present, a look-up-table (LUT) based pre-distortion is adopted in long-haul high-speed scenarios through searching the table by the pattern indexes trained before [20].

2) RECEIVER SIDE
a: EQUALIZATION
According to time-varying or not, the equalization can be divided into static equalization and adaptive equalization. Static equalization can further aim at linear and nonlinear impairments like CD and fiber nonlinearity, respectively. In nonlinear compensation, the maximum a posteriori (MAP) estimation is widely applied in the high-speed system, based on the strong data dependency of the channel nonlinearity [21]. Compared to the most investigated digital back prop-agation, it has the advantage of reducing computation.

Meanwhile the adaptive equalization is used for dynamic impairments compensations. The cascade multi-modulus algorithm (CMMA) combined with the decision-directed least-mean-square algorithm (DD-LMS) is a sufficient option to eliminate waveform distortion and compensate PMD for high-order QAM formats [20].

b: FREQUENCY OFFSET AND CARRIER PHASE ESTIMATION
The frequency offset is caused by the unlocked frequencies between the LO and transmitter, while the phase noise mainly originates from the laser linewidth. As both of them cause the constellation rotation, similar methods can be used for their compensation. Multi-stage estimation (MSE) is under great consideration for high-order QAM transmission, combining a coarse and a fine estimation [22]. After performing 4th power operation in the first stage, the second stage is followed using blind phase search (BPS) or maximum likelihood (ML) to get fine estimation. The pilot symbol based method can also be applied in the first stage to achieve a better tolerance but requires additional OH.

c: OTHER ESTIMATIONS
Especially in the high-baud-rate systems, some other estima-tions are applied to mitigate the bandwidth limitation of the

EO/OE devices. The partially-response maximum likelihood sequence estimation (PR-MLSE) is a power method using a partial response equalizer and a 4-state MLSE [23]. Together with the pre-emphasis, the ISI can be effectively reduced in high-baud-rate systems.

C. ULTRAHIGH-ORDER QAM TRANSMISSION
With the increase of the QAM order, the system poses higher requirements for the linewidth of the lasers, the noise figure of the amplifiers and the number of bits of the AWG. For the 3 GBd 4096-QAM demonstration, the linewidth of the laser is 4 kHz, and a 12 bits AWG is used to generate multi-level signals for each IQ channel [14]. It is worth noted that for ultrahigh-order QAM signals, optical phase lock loop (OPLL) is generally needed as shown by the dotted lines in Fig. 4. At the Rx-side, the phase of the LO is locked with the incoming signal source through a OPLL to mitigate the phase noise.

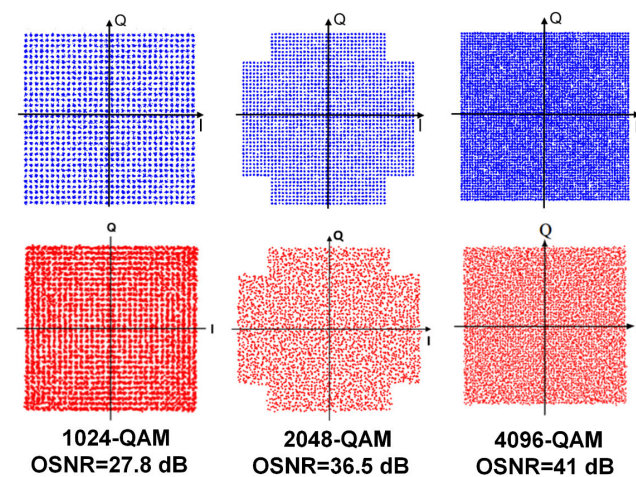| 1024-QAM | 2048-QAM | 4096-QAM |
| OSNR=27.8 dB | OSNR=36.5 dB | OSNR=41 dB |

FIGURE 5. Transmission performance of 1024-QAM, 2048-QAM and 4096-QAM over 150 km, 150 km, and 160 km, respectively [14], [24], [25].

Fig. 5 lists the constellations of three ultrahigh-order QAM signals: 1024-QAM, 2048-QAM and 4096-QAM, all

operating at 3 GBd [14], [24], [25]. The bottom constellations with red points represent the transmission performance of each QAM formats. The top constellations with blue points are their corresponding results we simulated for the back to back performance under the same devices conditions and baud rate. The constellations show that the higher the QAM order, the more sensitive it is to the transmission impairments. With the increasing QAM orders, the system requires higher OSNR. For 4096-QAM, to meet the pre-FEC BER of 2×10^{-2} using 20% OH, the OSNR after 160 km transmission needs to be greater than 38 dB [14]. While for 1024-QAM, a 27.8 dB OSNR is enough after 150 km transmission even adopting 7% OH [24].

Unless OSNR is further enhanced like reducing the noise figure of the amplifiers, it is difficult to achieve higher-order QAM transmission.

III. HIGH-BAUD-RATE SIGNAL GENERATION

In order to generate the high-baud-rate signal under the limited bandwidth of commercial EO/OE devices, several typical methods of high-baud-rate generation have been widely investigated to break the limitation, including electronic time-division multiplexing (ETDM), high-speed DAC, multiple spectral slices synthesis multiplexing and digital bandwidth interleaving (DBI) [13], [26]–[34]. At present, the first two high-baud-rate high-order QAM generation schemes are more commonly used because of their relatively simple structures.

A. ELECTRONIC TIME-DIVISION MULTIPLEXING

Along with the innovations in EO processing components, the preferred commercial method for high baud rate remains ETDM. Fig. 6(a) shows a common transmitter setup of ETDM, in which an optical carrier is provided by an external cavity laser (ECL). Pseudorandom bit sequences (PRBS) are generated at *X* Gb/s and multiplexed to *8X* Gb/s using two pairs of electronic multiplexers (MUX). Then an *8X* GBd QPSK is generated through an IQ modulator (IQM). By adding attenuators, this method can also generate other QAM signals. For a 16-QAM, two 6 dB attenuators are used after one MUX, and mixed with the signals of the other MUX to generate two 4 level signals [26].

To meet the needs for higher baud rate, two kinds of structures are commonly used: 4:1 MUX and 2:1 MUX, based on silicon germanium (SiGe) and indium phosphide (InP) technologies [27]. By adopting the packaged 2:1 InP double heterojunction bipolar transistor (InP-DHBT) selectors, the all-ETDM record-high 180 GBd PDM-QPSK was successfully generated and transmitted over 4480-km standard single mode fiber [28].

B. HIGH-SPEED DIGITAL TO ANALOG CONVERTER

Based on the common definition, DAC is acting as a different technology from ETDM in signal generation. High-speed DACs are effective in coherent optical systems because of utilizing less components for lower loss [29]. Fig. 6(b) depicts

a schematic of a 2^n-QAM transmitter using high-speed DACs. Two *nX* Gb/s PRBSs are fed into two DACs to generate $(2^n)^{0.5}$ level electrical signals. Then a carrier from a tunable ECL is separated into two lanes and modulated by the coming driving signals through an IQM.

High-order QAM could be generated by two multi-level DACs without changing the structure, while the sampling rate and the ENOB are thus considered as the limitations. The current DACs can provide sampling rates over 100 GSample/s, adopting different technologies like complementary metal oxide semiconductor (CMOS), InP and bipolar complementary metal oxide semiconductor (BiCMOS). Among them, BiCMOS shows a good performance and allows for direct connection with the DSP. In 2017, the SC PDM-64-QAM signal at 100 GBd (1Tb/s) was successfully implemented by employing BiCMOS DACs operating at 100 GSample/s. After transmitting over 306 km of large effective area fiber, the BER is well below the threshold using 20% OH [30].

C. MULTIPLE SPECTRAL SLICES SYNTHESIS MULTIPLEXING

Another effective approach based on spectral synthesis has been proposed through a novel structure splitting the optical spectrum. The transmitter setup is described in Fig. 6(c). In the digital domain, the spectrum of a high-speed signal is divided into *n* slices with equal width. In the optical domain, the light from an ECL passes through a pulse carver and is filtered out to *n* lines from an optical filter. The divided signals are delivered to *n* sets of IQMs, modulating the filtered carriers. By utilizing an optical delay line (DL) for each path, the spectral slices are synchronized before recombining. Finally, a high-baud-rate SC signal is achieved by composing these *n* slices through an optical combiner.

The generated QAM order depends on the bit resolution of DACs. With Nyquist pulse shaping, a SC PDM-16-QAM signal up to 127.9 GBd was well synthesized and transmitted over 3000 km, achieving a record 1 Tb/s line rate [31].

D. DIGITAL BANDWIDTH INTERLEAVING

Although all-electronically multiplexed high-speed high-order QAM signals over 100 GBd have been demonstrated in the laboratory, increasing the speed and bandwidth of a single multiplexer or DAC to even higher has proven to be difficult [32]. Through extending the analog bandwidth of DAC, DBI is an alternative approach to solve the problem [33]. The main idea of DBI is to split a wide-band signal into several narrower bands in the digital domain as if the signal is generated from one single wide-band DAC. Fig. 6(d) shows the architecture of a DBI-based DAC. The wide-band signal is first digitally cut into three slices which are low-frequency (LF), medium-frequency (MF), and high-frequency (HF). The seed tones with two frequency components are generated by an extra DAC. They are synchronized with other signals and up-converted for the MF and HF bands, respectively. This requires the complex conjugate MF spectrum generated by
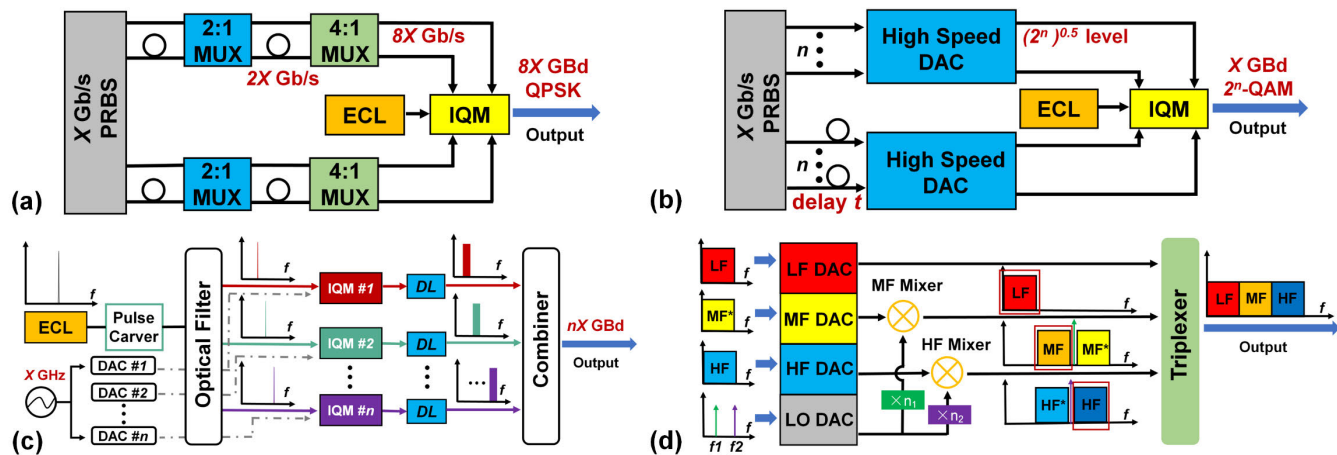
FIGURE 6. Architectures of different high-baud-rate high-order QAM generation schemes: (a) All-ETDM, (b) High-speed DAC, (c) Multiple spectral slices synthesis multiplexing and (d) DBI.
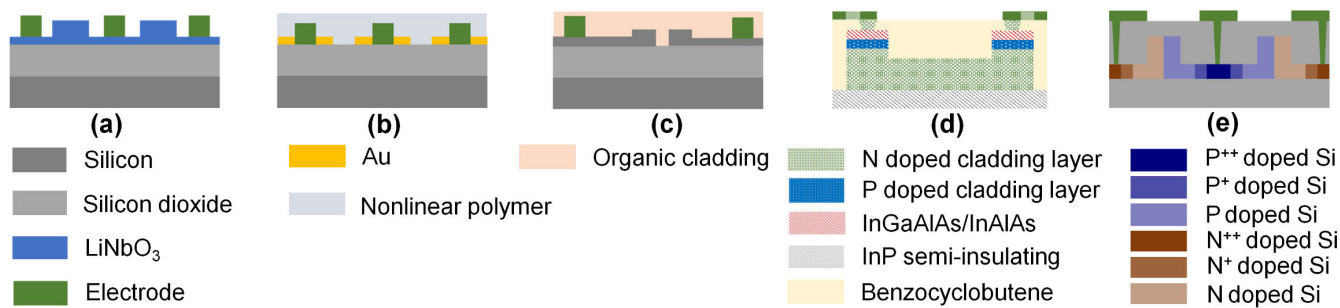

FIGURE 7. Typical modulators based on different materials: (a) Thin-film LiNbO₃, (b) Plasmonic, (c) SOH, (d) InP and (e) All-silicon.

the corresponding DAC. After passing through a triplexer, a wide-band signal output is finally synthesized.

A 240 GSample/s 100 GHz DBI-based DAC was successfully demonstrated and an all-electronically 180 GBd QPSK was further generated and detected [34]. At present, several other bandwidth multiplexing methods are demonstrated like Digital-Preprocessed Analog-Multiplexed DAC (DP-AM-DAC) [35]. This method uses an analog multiplexer (AMUX) instead of the mixers used in DBI, generating the current highest 192 GBd [13].

IV. HIGH-EFFICIENCY EO MODULATORS

After being able to successfully generate a high-baud-rate signal, modulation is another faced key limitation in implementing a high-baud-rate system. Recent progress in various EO modulators provides the potential possibility of realizing higher baud rate. According to the materials, EO modulators are mainly categorized into lithium niobite (LiNbO₃) modulators, plasmonic modulators, polymer modulators, InP modulators and all-silicon modulators. The modulation mechanism of these materials are mostly based on the linear EO effect, which changes the refractive index of the material in terms of the applied electrical signal, and further control the phase of the light that propagates through. Mach-Zehnder

modulators (MZM) is the most widely used structure in commercial coherent optical system. It consists of two phase modulators and could achieve the conversion from phase modulation to intensity modulation, as a result of constructive or destructive interference while working at the push-pull mode.

A. LiNbO₃ MODULATOR

LiNbO₃ is the most mature EO material with large bandwidth, low half-wave voltage (V_π), low optical loss and good linear EO properties [36]. However, due to its weak optical confinement, the conventional LiNbO₃ modulator is usually bulky and difficult to be integrated.

Recently, an emerged LiNbO₃-on-insulator platform provides a new way to break through the challenge in integration [37]. In this method, a LiNbO₃ film is bonded on top of a low-index substrate, then the waveguides are created by dry etching the LiNbO₃ layer. In 2018, an integrated thin-film LiNbO₃ modulator has been demonstrated with a bandwidth larger than 100 GHz, optical insertion loss lower than 0.1 dB, and electrode length less than 0.5 cm [38]. Using the MZM structure as shown in Fig. 7(a), the modulation of a 210 Gb/s amplitude shift keying signal was successfully

achieved, showing that the thin-film LiNbO$_3$ modulators can satisfy for power-efficient and high-speed applications.

B. PLASMONIC MODULATOR

Plasmonics is the technique of controlling and detecting surface plasmon polariton (SPP). In plasmonics, light is first converted into SPP, then the surface wave propagates at the metal-dielectric interface [39].

Since the 1980s, novel plasmonic modulators have started to debut, which have been demonstrated with compact footprints, low power consumption, and large bandwidth up to hundreds of gigahertz [40]. A typical plasmonic phase modulator shown in Fig. 7(b) consists of two metallic electrodes forming a metal-insulator-metal slot waveguide filled with a nonlinear organic material. A strip waveguide is used to feed light to the plasmonic slot waveguide and a taper transforms the light to a SPP. After modulated by the coming signal, the SPP is coupled back to the waveguide. Because of the small RC time constant, the bandwidth of the modulator is ultra-broad and flat. In 2019, a plasmonic MZM with bandwidth up to 500 GHz and a short length of 25 μm were experimentally demonstrated [41].

C. POLYMER MODULATOR

Polymer modulator has been investigated for many years due to fast EO response and lower cost. According to the different characteristics of modulators, they are classified into different types like all-polymer waveguide modulator, sol-gel waveguide modulator and polymer-silicon hybrid modulator [42]–[44].

Due to the inherent limitations of the single material modulator and the requirement of integration, the research on polymer-silicon modulator has gradually become a hotspot, especially the silicon-organic hybrid (SOH) modulators. For an SOH phase modulator whose typical structure is depicted in Fig. 7(c), the optical field is guided by a silicon waveguide, while the EO effect is provided by an organic cladding. An SOH phase modulator with a 3-dB bandwidth of at least 100 GHz was first demonstrated in 2014 [44]. The length of the device is around 0.5 mm and the voltage-length product is 11 V·mm. Such characteristics were very competitive among the available modulators.

D. InP MODULATOR

InP modulators mostly adopt multiple quantum well structure with high modulation efficiency and low driving voltage, making it compact and easy to integrate. But the high series resistance of the semiconductor is becoming a problem towards higher-baud-rate systems.

Optimizing its structure may be the key to overcome the problem. In 2017, an ultrahigh bandwidth MZM with a 3-dB bandwidth over 67 GHz was reported [45]. A low optical loss of 2 dB and a low V$_\pi$ of 1.5 V were achieved by employing a new n-i-p-n structure shown in Fig. 7(d). A p-type thin layer is added to the previous n-i-n structure, allowing the electric field to be applied more efficiently to the non-doped i-type

layer. The top n-type layer uses a reverse trapezoid to reduce the contact resistance. Two years later, the modulator employing the same structure achieved bandwidth up to 80 GHz, which is the best InP-based modulation performance reported so far [46].

E. ALL-SILICON MODULATOR

Compared with other materials, all-silicon modulator has the greatest advantage to integrate in a CMOS chip with other optical and electrical components. The small size and excellent compatibility make it stand out in integrated optics [47].

All-silicon MZM based on carrier depletion could be the most cost-efficient in commercial applications, whose typical structure is shown in Fig. 7(e). However, it is a challenge to achieve high efficient modulation in high-baud-rate systems, limited by carrier diffusion and weak EO linearity. The use of p+ and n+ doped layers can reduce electrical contact resistance and avoid high optical loss from the p++ and n++ layers. The loss imbalance between the phase shifters can also be alleviated to get a higher extinction ratio (ER). Higher bandwidth can be obtained by increasing the bias voltage and reducing the doping concentration, but at the cost of modulation efficiency. By implementing mid doping, an all-silicon modulator with high ER of 25 dB, a low V$_\pi$ of 4.1 V, and a bandwidth of 21 GHz was demonstrated [48].

F. COMPARISON OF DIFFERENT MATERIALS

Generally speaking, to achieve high-baud-rate modulation, a larger bandwidth of modulator is needed, but it also means a larger V$_\pi$. Thus, there is usually a trade-off between 3-dB bandwidth and V$_\pi$ in most cases, as shown in Fig. 8. It is observed that for the achievable bandwidth per volt, the thin-film LiNbO$_3$ and InP with around 50 GHz/V have great potential in high-baud-rate systems.
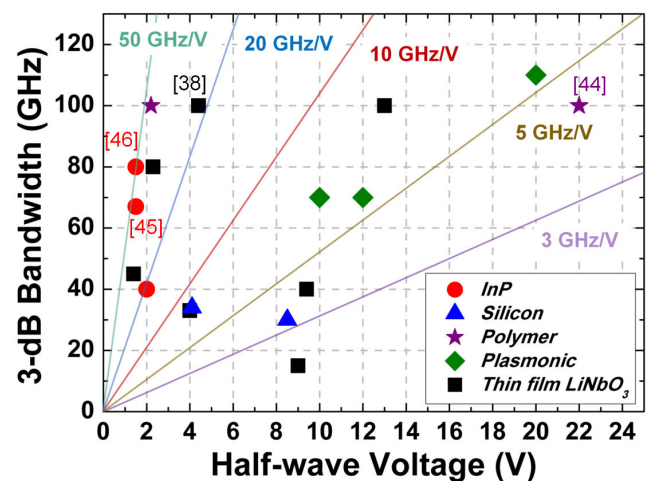
FIGURE 8. Comparison of 3-dB bandwidth and half-wave voltage of different materials.

In addition, comparison of key metrics of EO modulators using different materials is also summarized in Fig. 9. Electrode length, 3-dB bandwidth, V$_\pi$, ER and optical loss are
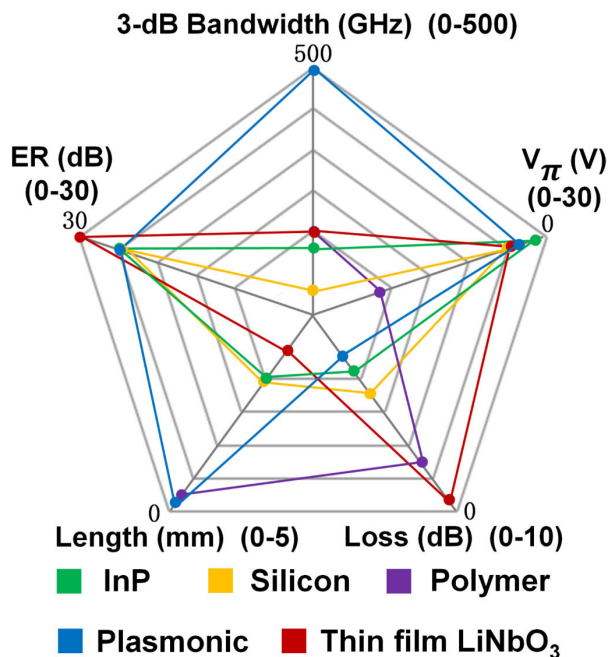
FIGURE 9. Comparison of key metrics of EO modulators of different materials.

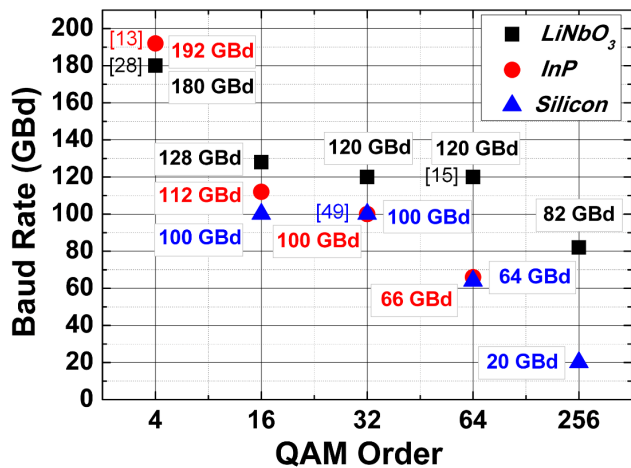**FIGURE 10.** The record high baud rate achieved by LiNbO₃, InP and Silicon of different QAM orders.

under consideration. For novel thin-film $LiNbO_3$ modulator, it has a better performance in bandwidth, loss and ER. But compared to other materials, the length of electrodes is still relatively large. Thus, further reducing the size of the modulator becomes a critical issue to be addressed. For plasmonic modulator, large bandwidth and compact size of the modulator have outstanding advantages. However, because of the interconversion of plasmonic and light, the loss of the modulator is the almost highest among these materials. For all-silicon modulator, the bandwidth and optical loss seem to be the critical obstacles. In high-speed systems, all-silicon modulators need to seek breakthroughs in these two aspects

to achieve effective integration. As for InP modulator, it has good performance in ER, V_π. But due to poor CMOS compatibility, there are shortcomings in terms of mass production and cost compared to all-silicon. Finally, as for polymer modulator, the parameters are not prominent but balanced. However, the modulators using organic materials have little chance for mass production, because of its sensitivity to oxygen atmosphere and risk of losing the poling when heated.

Among them, MZM modulators based on $LiNbO_3$, InP and all-silicon have been commercially used. The modulation performance of different QAM orders are listed in Fig. 10. With superb EO properties, $LiNbO_3$ modulators show clear advantages in different QAM orders. While with the structure optimized, the performance of the InP modulators gradually improves. The highest 192 GBd SC QPSK signal was generated using InP n-i-p-n heterostructure recently [13]. Although the EO properties of silicon are not as good as the other two, its potential high integration makes it widely applied. At present, 100 GBd 32-QAM signal employing all-silicon modulator was successful generated, achieving a net data rate of 416.7 Gb/s with pre-compensation and Rx-side DSP [49].

V. SYSTEM TRANSMISSION PERFORMANCE

When there are the proper generation methods and device conditions to support, it becomes meaningful to further investigate the performance of high-order QAM formats in high-baud-rate systems.

In general, QPSK, 16-QAM and 64-QAM are three commonly considered formats for commercial deployment. There are different options for applications with various distances and capacities. The trade-off between the increasing baud rate and QAM orders on the distance could offer some references for practical high-speed applications. The system we used in the simulations is similar to the Fig. 4 and some chosen basic parameters listed in TABLE 1, where BR stands for baud rate. Our simulated SC PDM systems consider all the typical fiber impairments. For different QAM formats, a set of optimized optical filter and Rx-side LPF bandwidths are selected. The pre-distortion is used in the Tx-side DSP, while the CD compensation, adaptive MIMO TDE and multi-stage (BPS and ML) phase recovery are adopted in the Rx-side DSP. For QPSK, CMA is selected in the adaptive TDE, while for the other formats, MMA is used for better compensation. The number of DSP taps is optimized individually for different QAM signals to achieve longest possible transmission distance. The 20% OH soft-decision FEC with a pre-FEC BER threshold of 2.4×10^{-2} is considered [50]. It is worth noting that, the performances of various devices, like DAC and laser, also have impacts under different circumstances. Here we focus on investigating the interrelation between QAM order and baud rate, and thus relatively good parameters of the individual components are chosen to minimize the impact accordingly. Furthermore, these parameters of the components used in the simulations are achievable in practice.

The relative reach of these QAM orders and baud rates for various SC capacities are depicted in Fig. 11(a). The

TABLE 1. Basic parameters used in simulations.

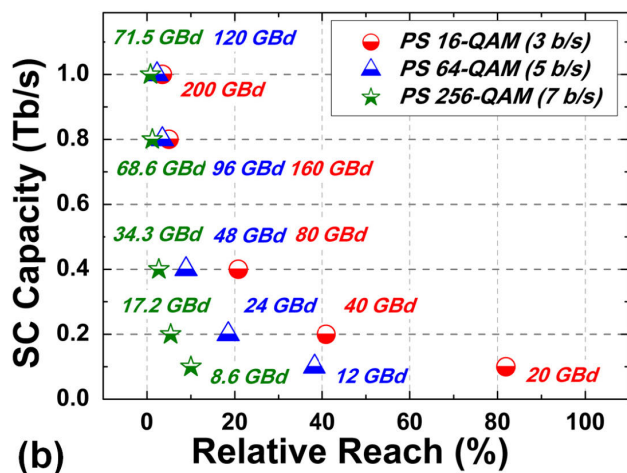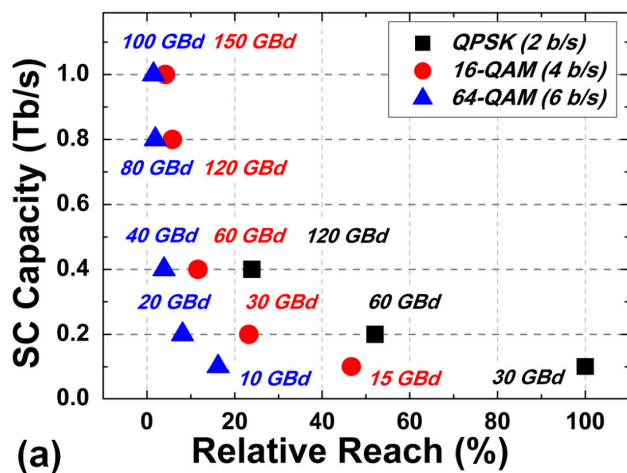| Parameters	Descriptions
laser & LO linewidth	1 kHz
laser & LO power	10 mW
roll of factor	0.2
MZM bandwidth	100 GHz
MZM extinction ratio	35 dB
transmitter output power	1 mW
optical filter bandwidth	1.5×BR
amplifier noise figure	4 dB
Rx-side LPF bandwidth	QPSK: 0.8×BR 16-QAM: 0.8×BR 64-QAM: 1.1×BR

FIGURE 11. The relative reach of different (a) uniform QAM and (b) probabilistic shaped QAM with baud rates aimed for SC 100 Gb/s, 200 Gb/s, 400 Gb/s, 800 Gb/s and 1 Tb/s (b/s: bits/symbol).

transmission distance of 30 GBd PDM-QPSK is considered as a reference for 100%. In the low capacity scenarios, PDM-QPSK shows significant advantage in the transmission distance, especially for 100 Gb/s and 200 Gb/s applications. For the same capacity, PDM-16-QAM can reach around half the

distance of PDM-QPSK, while PDM-64-QAM can achieve only a third of the distance of PDM-16-QAM. Meanwhile, for the same QAM orders, doubling the baud rate results in nearly half of the distance reduction. That means as the capacity increases, the distance advantages brought by lower orders will gradually mitigate. At 400 Gb/s, the transmission distance of 120 GBd PDM-QPSK is more close to 60 GBd PDM-16-QAM, while the latter saves half the bandwidth. At higher capacities, the advantages of high-order QAM formats are more obvious. For applications of 800 Gb/s and above, the SC PDM-QPSK requires baud rate exceeding 240 GBd, which is not achieved at present. Therefore, it can be analyzed that for long-haul or low-speed scenarios, PDM-QPSK is more effective, while for short-reach or applications above SC 800 Gb/s, PDM-16-QAM and PDM-64-QAM would be better choices because of their lower bandwidth requirements.
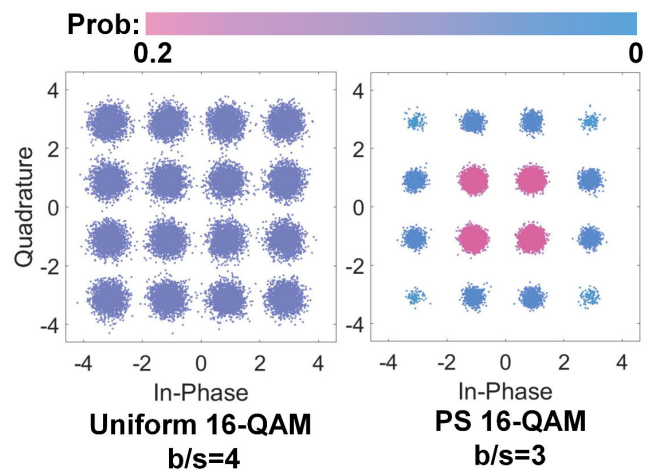

FIGURE 12. The concept of probabilistic shaped 16-QAM and corresponding uniform 16-QAM (b/s: bits/symbol; Prob: Probability).

In recent years, PS has attracted significant attention combined with various high-order QAM formats to approach the Shannon limit and extend the transmission distance [51]. In the bandwidth-limited additive white Gaussian noise (AWGN) channel, high-order QAM with uniformly distributed symbols exhibited an asymptotic loss of 1.53 dB compared to Shannon limit. PS shapes the probability of occurrence of the constellation points to approximate Gaussian signaling to overcome the limitation, as shown in Fig. 12. It alleviates the impact of channel impairments on QAM constellations, making higher-order QAM signals have the potential to be applied. By adopting the same system parameters in TABLE 1, we take the higher-order PDM-256-QAM into account in the simulations, and also considering 20% OH SD-FEC. Here, we choose the widely used Maxwell-Boltzmann (MB) distribution, making the achievable information rate (AIR) 3, 5 and 7 bits/symbol for 16-QAM, 64-QAM and 256-QAM, respectively. For an obvious comparison, we still take the transmission distance of 30 GBd PDM-QPSK as 100% for reference. Compared with the results in Fig. 11(a), at the same SC net data rate (<800 Gb/s), the transmission distance of PDM-16-QAM

and PDM-64-QAM with PS is nearly double that of the uniform ones, as shown in Fig. 11(b). However, using PS requires higher baud rate for a given data rate, thus the restrictions brought by higher baud rate have gradually become more prominent as the capacity increases. Especially for PDM-16-QAM, a baud rate higher than 160 GBd is required to achieve above 800 Gb/s. In this case, the distance advantage brought by PS is less obvious. So it can be analyzed that for applications below SC 400 Gb/s, PS PDM-16-QAM would be a competitive choice, while in the face of higher-speed requirements, it is more effective to adopt higher-order PS QAM formats with much lower baud rate.

VI. CONCLUSION

In this review, we have surveyed the recent progress of the enabling technologies in high-baud-rate coherent optical communication systems. High-order QAM signals with various advanced DSP algorithms have the great potential for achieving high-speed systems. To date, the bandwidth of the devices at the Tx-side is still limited, such as DAC and MUX. Thus four typical methods to generate high baud rate have emerged as needed. Then, to be able to modulate high-baud-rate signals, various modulators are flourishing. LiNbO$_3$ modulator is still one of the most competitive option in commercial applications. Especially the recent research of LiNbO$_3$ film is more promising to achieve breakthroughs in integrated optical systems. Plasmonic modulator shows great potential in large bandwidth, but the loss introduced by conversion between SPP and light is the problem need to be solved urgently. Meanwhile, all-silicon modulator is more suitable for monolithic integration, but the limited bandwidth would be an obstacle. As the current high-baud-rate systems and devices like pluggable transponders are moving towards higher-level integration, these three modulators might have broad prospects. Because increasing QAM orders and baud rates both limit system performance, there is usually a trade-off according to the applications with different distances and capacities. As a newly emerged method to extend the transmission distance, PS also provides a new direction for improving the performance of high-baud-rate systems. For the coming 800 GbE or even 1.6 TbE, PDM-64-QAM might be a better choice. By adopting PS, extended transmission distance can be achieved with additional bandwidth. Furthermore, higher-order QAM formats like PDM-256-QAM can also be considered for commercial system applications.

REFERENCES

[1] K. C. Kao and G. A. Hockham, "Dielectric-fibre surface waveguides for optical frequencies," *Proc. Inst. Electr. Eng.*, vol. 113, no. 7, pp. 1151–1158, Jul. 1966.

[2] H. Chen, C. Jin, B. Huang, N. K. Fontaine, R. Ryf, K. Shang, N. Grégoire, S. Morency, R.-J. Essiambre, G. Li, Y. Messaddeq, and S. LaRochelle, "Integrated cladding-pumped multicore few-mode erbium-doped fibre amplifier for space-division-multiplexed communications," *Nature Photon.*, vol. 10, no. 8, pp. 529–533, Aug. 2016.

[3] E. Desurvire, J. R. Simpson, and P. C. Becker, "High-gain erbium-doped traveling-wave fiber amplifier," *Opt. Lett.*, vol. 12, no. 11, pp. 888–890, Nov. 1987.

[4] R. A. Linke and A. H. Gnauck, "High-capacity coherent lightwave systems," *J. Lightw. Technol.*, vol. 6, no. 11, pp. 1750–1769, Nov. 1988.

[5] D.-S. Ly-Gagnon, S. Tsukamoto, K. Katoh, and K. Kikuchi, "Coherent detection of optical quadrature phase-shift keying signals with carrier phase estimation," *J. Lightw. Technol.*, vol. 24, no. 1, pp. 12–21, Jan. 2006.

[6] J. Zhang and J. Yu, "Generation and transmission of high symbol rate single carrier electronically time-division multiplexing signals," *IEEE Photon. J.*, vol. 8, no. 2, pp. 1–6, Apr. 2016.

[7] S. G. Evangelides, L. F. Mollenauer, J. P. Gordon, and N. S. Bergano, "Polarization multiplexing with solitons," *J. Lightw. Technol.*, vol. 10, no. 1, pp. 28–35, Jan. 1992.

[8] A. Matsushita, M. Nakamura, F. Hamaoka, S. Okamoto, and Y. Kisaka, "High-spectral-efficiency 600-Gbps/carrier transmission using PDM-256QAM format," *J. Lightw. Technol.*, vol. 37, no. 2, pp. 470–476, Jan. 15, 2019.

[9] F. Hamaoka, M. Nakamura, S. Okamoto, K. Minoguchi, T. Sasai, A. Matsushita, E. Yamazaki, and Y. Kisaka, "Ultra-wideband WDM transmission in S-, C-, and L-bands using signal power optimization scheme," *J. Lightw. Technol.*, vol. 37, no. 8, pp. 1764–1771, Apr. 15, 2019.

[10] Y. Liu, K. Xu, S. Wang, W. Shen, H. Xie, Y. Wang, S. Xiao, Y. Yao, J. Du, Z. He, and Q. Song, "Arbitrarily routed mode-division multiplexed photonic circuits for dense integration," *Nature Commun.*, vol. 10, no. 1, p. 3263, Dec. 2019.

[11] D. J. Richardson, J. M. Fini, and L. E. Nelson, "Space-division multiplexing in optical fibres," *Nature Photon.*, vol. 7, no. 5, pp. 354–362, May 2013.

[12] J. Wei, Q. Cheng, R. V. Penty, I. H. White, and D. G. Cunningham, "400 gigabit Ethernet using advanced modulation formats: Performance, complexity, and power dissipation," *IEEE Commun. Mag.*, vol. 53, no. 2, pp. 182–189, Feb. 2015.

[13] M. Nakamura, F. Hamaoka, M. Nagatani, Y. Ogiso, H. Wakita, H. Yamazaki, T. Kobayashi, M. Ida, H. Nosaka, and Y. Miyamoto, "192-Gbaud signal generation using ultra-broadband optical frontend module integrated with bandwidth multiplexing function," in *Proc. OFC*, San Diego, CA, USA, 2019, pp. 1–3, Paper Th4B.4.

[14] M. Terayama, S. Okamoto, K. Kasai, M. Yoshida, and M. Nakazawa, "4096 QAM (72 Gbit/s) single-carrier coherent optical transmission with a potential SE of 15.8 bit/s/Hz in all-Raman amplified 160 km fiber link," in *Proc. OFC*, San Diego, CA, USA, 2018, pp. 1–3, Paper Th1F.2.

[15] M. Nakamura, F. Hamaoka, M. Nagatani, H. Yamazaki, T. Kobayashi, A. Matsushita, S. Okamoto, H. Wakita, H. Nosaka, and Y. Miyamoto, "1.04 Tbps/carrier probabilistically shaped PDM-64QAM WDM transmission over 240 km based on electrical spectrum synthesis," in *Proc. OFC*, San Diego, CA, USA, 2019, pp. 1–3, Paper M4I.4.

[16] H.-G. Bach, A. Beling, G. G. Mekonnen, R. Kunkel, D. Schmidt, W. Ebert, A. Seeger, M. Stollberg, and W. Schlaak, "InP-based waveguide-integrated photodetector with 100-GHz bandwidth," *IEEE J. Sel. Topics Quantum Electron.*, vol. 10, no. 4, pp. 668–672, Jul. 2004.

[17] *Eospace 2019 Advanced Products, USA*. Accessed: Jun. 18, 2020. [Online]. Available: https://static1.squarespace.com/static/5b4391a0a277-2c7a5b0dae43/t/5c7428710d9297191c6942fe/1551116402875/EOSPACEbriefProductInfo2019.pdf

[18] D. Rafique, T. Rahman, A. Napoli, and B. Spinnler, "Digital pre-emphasis in optical communication systems: On the nonlinear performance," *J. Lightw. Technol.*, vol. 33, no. 1, pp. 140–150, Jan. 1, 2015.

[19] A. Napoli, M. M. Mezghanni, S. Calabro, R. Palmer, G. Saathoff, and B. Spinnler, "Digital predistortion techniques for finite extinction ratio IQ Mach–Zehnder modulators," *J. Lightw. Technol.*, vol. 35, no. 19, pp. 4289–4296, Oct. 1, 2017.

[20] J. Zhang, J. Yu, and H.-C. Chien, "High symbol rate signal generation and detection with linear and nonlinear signal processing," *J. Lightw. Technol.*, vol. 36, no. 2, pp. 408–415, Jan. 15, 2018.

[21] J.-X. Cai, Y. Cai, C. R. Davidson, D. G. Foursa, A. Lucero, O. Sinkin, W. Patterson, A. Pilipetskii, G. Mohs, and N. S. Bergano, "Transmission of 96 × 100-Gb/s bandwidth-constrained PDM-RZ-QPSK channels with 300% spectral efficiency over 10610 km and 400% spectral efficiency over 4370 km," *J. Lightw. Technol.*, vol. 29, no. 4, pp. 491–498, Feb. 15, 2011.

[22] M. S. Faruk and S. J. Savory, "Digital signal processing for coherent transceivers employing multilevel formats," *J. Lightw. Technol.*, vol. 35, no. 5, pp. 1125–1141, Mar. 1, 2017.

[23] J. Zhang, J. Yu, B. Zhu, and H.-C. Chien, "WDM transmission of single-carrier 120-GBd ETDM PDM-16QAM signals over 1200-km terrestrial fiber links," *J. Lightw. Technol.*, vol. 35, no. 4, pp. 1033–1040, Feb. 15, 2017.

[24] Y. Koizumi, K. Toyoda, M. Yoshida, and M. Nakazawa, "1024 QAM (60 Gbit/s) single-carrier coherent optical transmission over 150 km," *Opt. Express*, vol. 20, pp. 12508–12514, May 2012.

[25] S. Beppu, K. Kasai, M. Yoshida, and M. Nakazawa, "2048 QAM (66 Gbit/s) single-carrier coherent optical transmission over 150 km with a potential SE of 15.3 bit/s/Hz," in *Proc. OFC*, San Diego, CA, USA, 2019, pp. 4960–4969, Paper W1A.6.

[26] J. Zhang, J. Yu, and H. Chien, "WDM transmission of 16-channel single-carrier 128-GBaud PDM-16QAM signals with 6.06 b/s/Hz SE," in *Proc. OFC*, Los Angeles, CA, USA, 2017, pp. 1–3, Paper Tu2E.5.

[27] E. Lach and K. Schuh, "Recent advances in ultrahigh bit rate ETDM transmission systems," *J. Lightw. Technol.*, vol. 24, no. 12, pp. 4455–4467, Dec. 2006.

[28] G. Raybon, A. Adamiecki, J. Cho, F. Jorge, A. Konczykowska, M. Riet, B. Duval, J.-Y. Dupuy, N. Fontaine, P. J. Winzer, S. Chandrasekhar, and X. Chen, "180-GBaud all-ETDM single-carrier polarization multiplexed QPSK transmission over 4480 km," in *Proc. OFC*, San Diego, CA, USA, 2018, pp. 1–3, Paper Th4C.3.

[29] C. Laperle and M. O'Sullivan, "Advances in high-speed DACs, ADCs, and DSP for optical coherent transceiver," *J. Lightw. Technol.*, vol. 32, no. 4, pp. 629–643, Feb. 15, 2014.

[30] K. Schuh, F. Buchali, W. Idler, T. A. Eriksson, L. Schmalen, W. Templ, L. Altenhain, U. Dümler, R. Schmid, M. Möller, and K. Engenhardt, "Single carrier 1.2 Tbit/s transmission over 300 km with PM-64 QAM at 100 GBaud," in *Proc. OFC*, Los Angeles, CA, USA, 2017, pp. 1–3, Paper Th5B.5.

[31] H. Mardoyan, R. Rios-Müller, M. A. Mestre, P. Jennevé, L. Schmalen, A. Ghazisaeidi, P. Tran, S. Bigo, and J. Renaudier, "Transmission of single-carrier Nyquist-shaped 1-Tb/s line-rate signal over 3,000 km," in *Proc. OFC*, Los Angeles, CA, USA, 2015, pp. 1–3, Paper W3G.2.

[32] C. Schmidt, C. Kottke, R. Freund, F. Gerfers, and V. Jungnickel, "Digital-to-analog converters for high-speed optical communications using frequency interleaving: Impairments and characteristics," *Opt. Express*, vol. 26, pp. 6758–6770, Mar. 2018.

[33] X. Chen, S. Chandrasekhar, S. Randel, G. Raybon, A. Adamiecki, P. Pupalaikis, and P. J. Winzer, "All-electronic 100-GHz bandwidth digital-to-analog converter generating PAM signals up to 190 GBaud," *J. Lightw. Technol.*, vol. 35, no. 3, pp. 411–417, Feb. 1, 2017.

[34] X. Chen, S. Chandrasekhar, P. Winzer, P. Pupalaikis, I. Ashiq, A. Khanna, A. Steffan, and A. Umbach, "180-GBaud Nyquist shaped optical QPSK generation based on a 240-GSa/s 100-GHz analog bandwidth DAC," in *Proc. ACP*, Wuhan, China, 2016, pp. 1–3, Paper AS4A.1.

[35] H. Yamazaki, M. Nagatani, S. Kanazawa, H. Nosaka, T. Hashimoto, A. Sano, and Y. Miyamoto, "Digital-preprocessed analog-multiplexed DAC for ultrawideband multilevel transmitter," *J. Lightw. Technol.*, vol. 34, no. 7, pp. 1579–1584, Apr. 1, 2016.

[36] M. He, M. Xu, Y. Ren, J. Jian, Z. Ruan, Y. Xu, S. Gao, S. Sun, X. Wen, L. Zhou, L. Liu, C. Guo, H. Chen, S. Yu, L. Liu, and X. Cai, "High-performance hybrid silicon and lithium niobate Mach–Zehnder modulators for 100 Gbit s^{-1} and beyond," *Nature Photon.*, vol. 13, no. 5, pp. 359–364, 2019.

[37] A. Boes, B. Corcoran, L. Chang, J. Bowers, and A. Mitchell, "Status and potential of lithium niobate on insulator (LNOI) for photonic integrated circuits," *Laser Photon. Rev.*, vol. 12, no. 4, Apr. 2018, Art. no. 1700256.

[38] C. Wang, M. Zhang, X. Chen, M. Bertrand, A. Shams-Ansari, S. Chandrasekhar, P. Winzer, and M. Loncar, "Integrated lithium niobate electro-optic modulators operating at CMOS-compatible voltages," *Nature*, vol. 562, no. 7725, pp. 101–104, Oct. 2018.

[39] A. Melikyan, L. Alloatti, A. Muslija, D. Hillerkuss, P. C. Schindler, J. Li, R. Palmer, D. Korn, S. Muehlbrandt, D. Van Thourhout, B. Chen, R. Dinu, M. Sommer, C. Koos, M. Kohl, W. Freude, and J. Leuthold, "High-speed plasmonic phase modulators," *Nature Photon.*, vol. 8, no. 3, pp. 229–233, 2014.

[40] J. Schildkraut, "Long-range surface plasmon electrooptic modulator," *Appl. Opt.*, vol. 27, no. 21, pp. 4587–4590, 1988.

[41] M. Burla, C. Hoessbacher, W. Heni, C. Haffner, Y. Fedoryshyn, D. Werner, T. Watanabe, H. Massler, D. L. Elder, L. R. Dalton, and J. Leuthold, "500 GHz plasmonic Mach–Zehnder modulator enabling sub-THz microwave photonics," *APL Photon.*, vol. 4, no. 5, May 2019, Art. no. 056106.

[42] H. Miura, F. Qiu, A. M. Spring, T. Kashino, T. Kikuchi, M. Ozawa, H. Nawata, K. Odoi, and S. Yokoyama, "High thermal stability 40 GHz electro-optic polymer modulators," *Opt. Express*, vol. 25, pp. 28643–28649, Nov. 2017.

[43] Y. Enami, A. Seki, S. Masuda, T. Joichi, J. Luo, and A. K.-Y. Jen, "Bandwidth optimization for Mach–Zehnder polymer/Sol–Gel modulators," *J. Lightw. Technol.*, vol. 36, no. 18, pp. 4181–4189, Sep. 15, 2018.

[44] L. Alloatti, R. Palmer, S. Diebold, K. P. Pahl, B. Chen, R. Dinu, M. Fournier, J.-M. Fedeli, T. Zwick, W. Freude, C. Koos, and J. Leuthold, "100 GHz silicon–organic hybrid modulator," *Light Sci. Appl.*, vol. 3, no. 5, p. e173, 2014.

[45] Y. Ogiso, J. Ozaki, Y. Ueda, N. Kashio, N. Kikuchi, E. Yamada, H. Tanobe, S. Kanazawa, H. Yamazaki, Y. Ohiso, T. Fujii, and M. Kohtoku, "Over 67 GHz bandwidth and 1.5 v vp InP-based optical IQ modulator with n-i-p-n heterostructure," *J. Lightw. Technol.*, vol. 35, no. 8, pp. 1450–1455, Apr. 15, 2017.

[46] Y. Ogiso, Y. Hashizume, H. Tanobe, N. Nunoya, M. Ida, Y. Miyamoto, M. Ishikawa, J. Ozaki, Y. Ueda, H. Wakita, M. Nagatani, H. Yamazaki, M. Nakamura, T. Kobayashi, and S. Kanazawa, "80-GHz bandwidth and 1.5-V vp InP-based IQ modulator," *J. Lightw. Technol.*, vol. 38, no. 2, pp. 249–255, Jan. 15, 2020.

[47] J. Witzens, "High-speed silicon photonics modulators," *Proc. IEEE*, vol. 106, no. 12, pp. 2158–2182, Dec. 2018.

[48] J. Zhou, J. Wang, L. Zhu, and Q. Zhang, "High baud rate all-silicon photonics carrier depletion modulators," *J. Lightw. Technol.*, vol. 38, no. 2, pp. 272–281, Jan. 15, 2020.

[49] S. Zhalehpour, J. Lin, M. Guo, H. Sepehrian, Z. Zhang, L. A. Rusch, and W. Shi, "All-silicon IQ modulator for 100 GBaud 32 QAM transmissions," in *Proc. OFC*, San Diego, CA, USA, 2019, pp. 1–3, Paper Th4A.5.

[50] D. Chang, F. Yu, Z. Xiao, Y. Li, N. Stojanovic, C. Xie, X. Shi, X. Xu, and Q. Xiong, "FPGA verification of a single QC-LDPC code for 100 Gb/s optical systems without error floor down to BER of 10^{-15}," in *Proc. OFC/NFOEC*, Los Angeles, CA, USA, 2011, pp. 1–3, Paper OTuN2.

[51] J. Cho and P. J. Winzer, "Probabilistic constellation shaping for optical fiber communications," *J. Lightw. Technol.*, vol. 37, no. 6, pp. 1590–1607, Mar. 15, 2019.

SI-AO LI received the B.S. degree in optical information science and technology from the Dalian University of Technology, Dalian, Liaoning, China, in 2018. He is currently pursuing the M.S. degree in optical engineering with the Institute of Modern Optics, Nankai University, Tianjin, China.

HAO HUANG (Member, IEEE) received the B.S. degree from Jilin University, Changchun, China, in 2006, the M.S. degree from the Beijing University of Posts and Telecommunications, Beijing, China, in 2009, and the Ph.D. degree in electrical engineering from the University of Southern California, Los Angeles, CA, USA, in 2014. He is currently working with Lumentum Operations LLC as a Hardware Engineer. He has coauthored more than 100 publications, including peer-reviewed journals and conference proceedings. His research areas include optical communication system and components, optical sensing systems, and digital signal processing. He is a member of the Optical Society of America (OSA).

ZHONGQI PAN (Senior Member, IEEE) received the B.S. and M.S. degrees from Tsinghua University, China, and the Ph.D. degree from the University of Southern California, Los Angeles, all in electrical engineering.

He is currently a Professor with the Department of Electrical and Computer Engineering. He also holds BORSF Endowed Professorship in Electrical Engineering II, and BellSouth/BORSF Endowed Professorship in Telecommunications. He has authored/coauthored 160 publications, including five book chapters and 18 invited presentations/articles. He holds five U.S. patents and one China patent. His research interests include photonics, including photonic devices, fiber communications, wavelength-division-multiplexing (WDM) technologies, optical performance monitoring, coherent optical communications, space-division-multiplexing (SDM) technologies, and fiber sensor technologies. Prof. Pan is a Senior Member of the Optical Society of America (OSA).

RUNZE YIN had an Internship at Nankai University for coherent optical systems. He is currently a Customer Quality Engineer involved in chip failure analysis at NXP Semiconductors, China.

YINGNING WANG received the B.S. degree in electronic science and technology from Shandong University, Qingdao, Shandong, China, in 2019. She is currently pursuing the M.S. degree in optical engineering with the Institute of Modern Optics, Nankai University, Tianjin, China.

YUXI FANG received the bachelor's degree in optical information science and technology from Anhui University, Hefei, Anhui, China, in 2018. She is currently a Graduate Student with the Institute of Modern Optics, Nankai University, Tianjin, China. Her research interest includes integrated optics.

YIWEN ZHANG received the B.S. degree in optical information science and technology from the Dalian University of Technology, Dalian, Liaoning, China, in 2018. She is currently pursuing the M.S. degree in optical engineering with the Institute of Modern Optics, Nankai University, Tianjin, China.

CHANGJING BAO (Member, IEEE) received the Ph.D. degree in electrical engineering from the University of Southern California, Los Angeles, CA, USA, in 2017. He has authored and coauthored more than 100 journal articles and conference proceedings. His research interests include optical communications, nonlinear optics, and integrated optics.

YONGXIONG REN (Member, IEEE) received the B.E. degree in communications engineering from the Beijing University of Posts and Telecommunications (BUPT), Beijing, China, in 2008, the M.S. degree in radio physics from Peking University (PKU), Beijing, in 2011, and the Ph.D. degree in electrical engineering from the University of Southern California (USC), Los Angeles, CA, USA, in 2016.

He has authored and coauthored more than 130 research articles with a Google Scholar citation number of >5500. His publications include 57 peer-reviewed journal articles, 76 international conference proceedings, one book chapter, and three patents. His main research interests include high-capacity free-space and fiber optical communications, millimeter-wave communications, space division multiplexing, orbital angular momentum multiplexing, atmospheric optics, and atmospheric turbulence compensation.

ZHAOHUI LI received the B.S. degree from the Department of Physics, Nankai University, Tianjin, China, in 1999, the M.Sc. degree from the Institute of Modern Optics, Nankai University, in 2002, and the Ph.D. degree from Nanyang Technological University, Singapore, in 2007. He is currently working as a Professor with the School of Electronics and Information Technology, Sun Yat-sen University, Guangzhou, China, in 2009. His research interests are optical communication systems, optical signal processing technology, and ultrafine measurement systems.

YANG YUE (Member, IEEE) received the B.S. and M.S. degrees in electrical engineering and optics from Nankai University, Tianjin, China, in 2004 and 2007, respectively, and the Ph.D. degree in electrical engineering from the University of Southern California, Los Angeles, CA, USA, in 2012.

He is currently a Professor with the Institute of Modern Optics, Nankai University. He has published over 150 peer-reviewed journal articles and conference proceedings, three edited books, one book chapter, >10 invited articles, >30 issued or pending patents, and >80 invited presentations. His current research interests include intelligent photonics, optical communications and networking, optical interconnect, detection, imaging and display technology, integrated photonics, free-space, and fiber optics.

Dr. Yue is a member of the IEEE Communications Society (ComSoc), IEEE Photonics Society (IPS), the International Society for Optical Engineering (SPIE), Optical Society of America (OSA), and the Photonics Society of Chinese-American (PSC). He is an Associate Editor of IEEE Access, and an Editor Board Member for three other scientific journals. He has served as the Guest Editor for six journal special issues, a committee member and a session chair for ~30 international conferences, and a reviewer for >50 prestigious journals and the OSA Centennial Special Events Grant 2016.

● ● ●